The Journal of Liquid Biopsy 4 (2024) 100143

Contents lists available at ScienceDirect

The Journal of Liquid Biopsy

journal homepage: www.sciencedirect.com/journal/the-journal-of-liquid-biopsy

NGS detection of gene rearrangements and METexon14 mutations in liquid biopsy of advanced NSCLC patients: A study of two Italian centers

Michela Verzè [a,b,1], Andrea Boscolo Bragadin [c,1], Roberta Minari [a], Giulia Pasello [d,e,*], Fabiana Perrone [a], Daniela Scattolin [d,e], Paola Bordi [a], Monica Pluchino [a,b], Alessandro Leonetti [a], Giulia Mazzaschi [a,b], Francesco Bonatti [a,b], Letizia Gnetti [f], Lorena Bottarelli [b], Elisabetta Zulato [c], Giorgia Nardo [c], Chiara Dalle Fratte [c], Alessia Padovan [c], Laura Bonanno [e], Marcello Tiseo [a,b,2], Stefano Indraccolo [c,d,2]

[a] Medical Oncology Unit, University Hospital of Parma, Parma, Italy
[b] Department of Medicine and Surgery, University of Parma, Parma, Italy
[c] Basic and Translational Oncology Unit, Veneto Institute of Oncology IOV – IRCCS, Padua, Italy
[d] Department of Surgery, Oncology and Gastroenterology, University of Padua, Padua, Italy
[e] Medical Oncology 2, Veneto Institute of Oncology IOV – IRCCS, Padua, Italy
[f] Pathology Unit, University Hospital of Parma, Parma, Italy

ARTICLE INFO

Keywords:
Liquid biopsy
ctDNA
Advanced NSCLC
Concordance rate
Gene rearrangements
METexon14 mutations

ABSTRACT

Introduction: ctDNA is a useful tool for NGS molecular profiling in advanced NSCLC patients. Its clinical applicability in patients with gene rearrangements is still limited due to a lower detection rate of these types of alterations compared to single SNVs or small indels. To this purpose, we performed a study in two Italian centers to assess the concordance between tissue and plasma samples in the detection of genes fusions (*ALK*, *ROS*, *RET*) and *METexon14* mutations in advanced NSCLC patients.

Methods: Patients with a histological diagnosis of oncogene addicted (*ALK*, *ROS1*, *RET* positive or *METexon14* mutated) advanced NSCLC were enrolled at the time of first line of TKI treatment. Plasma samples were harvested before the start of TKI treatment and NGS analysis on ctDNA samples using the AVENIO ctDNA Expanded kit was performed. The Positive Percent Agreement (PPA) between tissue and plasma was calculated.

Results: Fifty-eight rearranged or *METexon14* mutated NSCLC patients were included and 57 ctDNA samples were successfully sequenced. An overall PPA of 37% (21/57) was obtained, with a best performance for *RET* fusion (80%), intermediate for *METexon14* skipping mutations (40%) and *ALK* rearranged (36%) and a worst one for *ROS1* rearranged samples (18%). We found *TP53*, *APC* and *SMAD4* as most prevalent co-mutated genes (21%, 12% and 10% of patients, respectively). Among different factors considered, increased driver detection rate in patients with extra-thoracic metastases ($p = 0.0049$) was observed. Significantly shorter survival was observed in patients harboring co-occurring *KRAS/NRAS* mutations in ctDNA.

Conclusions: ctDNA testing to detect oncogenic fusions or *METexon14* mutations in advanced NSCLC patients is useful, even if type of gene alterations and clinical characteristics could influence the driver detection rate. Liquid biopsy represents a complementary tool to tissue genotyping, however more sensitive approaches for gene fusions and *METexon14* detection are needed to implement its strength and reliability.

1. Introduction

Lung cancer is the first cause of cancer-related death in the

* Corresponding author. Department of Surgery, Oncology and Gastroenterology, University of Padua and Medical Oncology 2, Veneto Institute of Oncology IOV – IRCCS, Padua, Italy.
E-mail address: giulia.pasello@unipd.it (G. Pasello).
[1] Equally contributed as first authors.
[2] Equally contributed as senior authors.

https://doi.org/10.1016/j.jlb.2024.100143
Received 24 January 2024; Received in revised form 1 February 2024; Accepted 2 February 2024

Abbreviations

(NSCLC) Non-small Cell Lung Cancer
(EGFR) Epidermal Growth Factor Receptor
(BRAF) B-Raf proto-oncogene,
(KRAS) Kirsten Rat Sarcoma Virus
(HER2) Human Epidermal Growth Factor Receptor 2
(MET) exon14 mutations MET proto-oncogene
(ALK) Anaplastic lymphoma kinase
(ROS1) c-ros oncogene 1 receptor tyrosine kinase
(NTRK) neurotrophic tyrosine kinase receptor
(RET) rearrangementsRearranged in transfection;
(PD-L1) Programmed death-ligand 1
(ESMO) European Society for Medical Oncology
(IASLC) International Association for the Study of Lung Cancer
(ctDNA) circulating tumor DNA
(cfDNA) cell-free DNA
(FDA) Food and Drug Administration
(GCP) Good Clinical Practice
(ctRNA) circulating tumor RNA
(TKI) Tyrosine Kinase Inhibitor
(BCL) Binary Base Call
(CNVs) Copy; Number Variations
(rt-PCR) real time-PCR
(PPA) Positive Percent Agreement
(PFS) Progression-Free Survival
(OS) Overall Survival
(ECOG) Eastern Cooperative Oncology Group
(PS) Performance Status
(SRV) Splice Region Variants
(AF) Allele Frequency
(mAF) mean AF
(SNVs) Single Nucleotide Variations
(TP53) Tumor Protein p53
(APC) Adenomatous Polyposis Coli
(SMAD 4) Mothers against decapentaplegic homolog 4
(NRAS) Neuroblastoma RAS viral oncogene
(TF) Tumor Fraction
(cfRNA) cell-free RNA

industrialized countries [1]. Over the past decade, lung cancer treatment landscape has substantially evolved due to introduction of immunotherapy and target therapy. In order to tailor treatment, increasing molecular information are necessary in advanced non-small cell lung cancer (NSCLC) patients. Indeed, European Society for Medical Oncology (ESMO) guidelines currently recommend testing at least Epidermal Growth Factor Receptor (*EGFR*), B-Raf proto-oncogene (*BRAF*), Kirsten Rat Sarcoma Virus (*KRAS*), Human Epidermal Growth Factor Receptor 2 (*HER2*) and MET proto-oncogene (*MET*) exon14 mutations, Anaplastic lymphoma kinase (*ALK*), The c-ros oncogene 1 receptor tyrosine kinase (*ROS1*), neurotrophic tyrosine kinase receptor (*NTRK*), Rearranged in transfection (*RET*) rearrangements and Programmed death-ligand 1 (*PD-L1*) expression levels in non-squamous advanced NSCLC and in young and/or never smoker patients with squamous histology [2].

Currently, tissue biopsy is the gold standard for diagnosis and molecular profiling in lung cancer, even if the material obtained from an invasive procedure could be inadequate or not sufficient for a complete molecular characterization. To overcome these limitations, liquid biopsy, defined as a minimally invasive technique allowing the detection, analysis and monitoring of cancer from different biofluids, could be a valid alternative. Plasma circulating tumor DNA (ctDNA), which corresponds to the tumoral fraction out of the total circulating-free DNA (cfDNA), is the most exploited analyte as clinical biomarker and its use has shown to improve the management of advanced NSCLC patients [3,4]. Based on these considerations, analysis of ctDNA is now recommended by the International Association for the Study of Lung Cancer (IASLC) when the tissue samples are unavailable, insufficient, or inadequate for a complete molecular profiling [5].

Next generation sequencing (NGS) that allows to simultaneously investigate the main classes of molecular alterations represents the standard technique for lung cancer molecular characterization and is applicable both on tissue and plasma/liquid samples [6,7]. In particular, in 2020, US Food and Drug Administration (FDA) approved two diagnostic Good Clinical Practice (GCP) ctDNA-based NGS tests for clinical practice: Guardant360® CDx (Guardant Health, Palo Alto, CA, USA) and FoundationOne® Liquid CDx (Foundation Medicine, Cambridge, MA, USA) [8,9].

Despite substantially increased NGS testing of ctDNA in advanced NSCLC, data on its clinical applicability in detection of gene rearrangements are limited. NGS detection of gene rearrangements and METexon14 mutations presents specific technical challenges, in particular in case of liquid biopsy and with samples with low ctDNA compared to cfDNA [10]. Considering that rearrangement breakpoints can occur inside intronic regions, the use of circulating tumor RNA (ctRNA) would perhaps be more appropriate, but its low amount and quality issues limit its exploitation in the diagnostics setting.

Considering this context and the growing use of NGS in lung cancer liquid biopsy in clinical practice, we proposed with this study to investigate the concordance between tissue and plasma samples in the detection of *ALK*, *ROS1* and *RET* rearrangements and METexon14 mutations in advanced NSCLC patients.

2. Materials and methods

2.1. Patients and plasma samples collection

We conducted a study including advanced NSCLC patients harboring a fusion of *ALK*, *ROS1* or *RET* genes or *METexon14* gene mutations detected on tumor tissue sample. Patients were prospectively enrolled in the DYNAMIC and LiMoRe studies performed by University Hospital of Parma (Parma, Italy) from November 2015 to August 2023 and in the ARMONY study promoted by Veneto Institute of Oncology (IOV, Padova, Italy) from December 2019 to July 2023. These studies were designed to investigate liquid biopsy in advanced NSCLC and, for the present analysis, the cohorts from the two Italian centers were merged. Eligibility criteria included confirmed histological diagnosis of advanced NSCLC with a driver oncogene fusion (*ALK*, *ROS1* and *RET*) or with a *METexon14* mutations detected in tumor tissue biopsy as per diagnostic routine and the enrollment at the time of first-line of specific Tyrosine Kinase Inhibitor (TKI) treatment. Patients' informed consent was obtained before enrollment in each study. All studies approved by Ethical Committee were conducted in accordance with the precepts of the Helsinki declaration.

Liquid biopsy was obtained for each patient before starting the TKI treatment and 20 mL of blood were collected into EDTA tubes at University Hospital of Parma or in Cell-Free DNA Blood Collection Tubes (cfDNA BCT; Streck Corporate, La Vista, NE, USA) at Veneto Institute of Oncology. Plasma was separated within 2 h from collection for EDTA or 24–72 h for cfDNA BCT tubes and stored at −80 °C until cfDNA extraction.

2.2. Extraction of cfDNA and assessment of its quantity and quality

In both centers cfDNA extraction was performed starting from 2.5 to 5 mL of plasma using the AVENIO cfDNA Isolation Kit (Roche Diagnostics, Basel, Switzerland), following manufacturer's instructions. cfDNA concentration was measured using the Qubit dsDNA High Sensitivity Assay Kit with Qubit 4 Fluorometer (Thermo Fisher Scientific, Waltham, MA, USA). cfDNA quality was determined using the cfDNA ScreenTape Assay with the Agilent 4200 TapeStation (Agilent Technologies, Santa Clara, CA, USA).

2.3. cfDNA sequencing with the AVENIO ctDNA expanded kit

NGS libraries were prepared starting from 10 to 50 ng of input cfDNA, using the AVENIO ctDNA Expanded kit (77 genes; Roche Diagnostics, Basilea, CHE), as described in the manufacturer's protocol. Final individual libraries were quantified with Qubit dsDNA HS Assay kit, and quality was determined using the Agilent High Sensitivity D1000 ScreenTape Assay with the Agilent 4200 TapeStation system. We pooled together 4 or 8 libraries and sequencing was performed using the NextSeq 500/550 Mid Output v2 kit (300 cycles) for a pool of 4 libraries or the NextSeq High Output kit (300 cycles) for a pool of 8, in paired-end mode (2×151 cycles).

2.4. NGS data analysis

Binary Base Call (BCL) files obtained from sequencing were sorted by index, aligned to human genome assembly hg38 and gene variants, fusions and copy number variations (CNVs) were called using the AVENIO ctDNA analysis software 2.0 (Roche Diagnostics). Variants present in the population database (1000 genomes) with allelic frequency >1%, synonymous variants and intronic variants were filtered out. Remaining variants were searched manually using Varsome Premium and classified according to ACGM and AMP score [11]. Only pathogenic, likely pathogenic and variants of unknown significance (VUS) were considered for this study.

2.5. Molecular diagnosis on tissue specimens

Tissue molecular characterization was performed as per diagnostic routine at the Pathological.

Anatomy Units of University Hospital of Parma and Veneto Institute of Oncology (IOV) using different methods such as immunohistochemistry, FISH, Sanger Sequencing, NGS and real time PCR (rt-PCR), allowing to investigate all the clinically relevant molecular alterations including *EGFR*, *BRAF*, *KRAS*, *HER2* and *METexon14* mutations, and *ALK*, *ROS1*, *NTRK*, *RET* rearrangements.

2.6. Statistical analysis

Statistical analyses were performed using GraphPad Statistical Software Version 9.5.0 (GraphPad Software, Boston, MA, USA) and Jamovi Statistical Software Version 2.3 (Sydney, Australia). Fisher's exact test and Mann-Whitney nonparametric test were used to examine the differences in categorical variables. Correlations between pre-analytical factors were calculated through Spearman correlation's test. Positive percent agreement (PPA) of NGS results between tissue and plasma was calculated. Median Progression-Free Survival (PFS) and Overall Survival (OS) were calculated using the Kaplan-Meier method and Cox's proportional hazards model. 95% CI was calculated with the Wald test. Differences in survival between groups were determined by Log rank test. All p-values were two sided and $p < 0.05$ was considered to indicate a statistically significant difference.

3. Results

3.1. Patients characteristics

From November 2015 to August 2023 58 patients affected by locally advanced or metastatic oncogene addicted (*ALK*, *ROS1* or *RET* positive or *METexon14* mutated) NSCLC were enrolled. Median age was 64 years (30–85). The majority of patients was female (63.8%) and never smoker (58.7%). Forty-nine (84.4%) patients had Eastern Cooperative Oncology Group (ECOG) Performance Status (PS) 0–1. At diagnosis, the stage of disease was advanced in 45 (77.6%) patients and the number of metastatic sites was more than three in 24 (41.4%) patients.

The tissue known driver alterations were: *ALK* rearrangements (37/58 patients; 63.9%), *ROS1* rearrangements (11/58 patients; 18.9%), *RET* fusions (5/58 patients; 8.6%), *METexon14* mutations (5/58 patients; 8.6%). Most patients (77.6%) received a target therapy as first-line treatment for advanced disease. *ALK* positive patients were treated with Alectinib in 31 cases and Crizotinib in 6; *ROS1* positive patients were treated with Crizotinib in 9 cases and Entrectinib in 2; *RET* positive patients were treated with Selpercatinib in 3 cases and Pralsetinib or

Table 1
Patients' main characteristics.

Clinicopathological variables	Patients (n = 58) n (%)
Age, years	64 (30–85)
Sex	
Male	21 (36.2)
Female	37 (63.8)
Smoking status	
Current	7 (12.0)
Former	17 (29.3)
Never	34 (58.7)
ECOG PS	
0	24 (41.3)
1	25 (43.1)
2	9 (15.6)
Stage at diagnosis	
II	2 (3.4)
III	11 (19.0)
IV	45 (77.6)
N. of Metastatic sites involved	
≤3	34 (58.6)
>3	24 (41.4)
N. of previous lines of therapy	
<1	45 (77.6)
≥ 1	13 (22.4)
Driver alteration	
ALK	37 (63.9)
ROS-1	11 (18.9)
RET	5 (8.6)
METexon14	5 (8.6)
Type of Molecular Testing (overall population)	
IHC	30 (51.7)
FISH	9 (15.6)
rtPCR	10 (17.2)
NGS	7 (12.1)
Sanger Sequencing	2 (3.4)
Type of Molecular Testing (by driver alteration)	
IHC	*ALK* (28/30); *ROS1* (2/30)
FISH	*ALK* (1/9); *ROS1* (7/9); *RET* (1/9)
rtPCR	*ALK* (7/10); *RET* (1/10); *METexon14* (2/10)
NGS	*ALK* (1/7); *ROS1* (2/7); *RET* (3/7); *METexon14* (1/7)
Sanger Sequencing	*METexon14* (2/2)
Drug administered	
Alectinib	32 (55.2)
Crizotinib	19 (32.7)
Selpercatinib	3 (5.3)
Entrectinib	2 (3.4)
Pralsetinib	1 (1.7)
Capmatinib	1 (1.7)

ECOG PS: Eastern Cooperative Oncology Group Performance status; IHC, Immunohistochemistry; FISH, Fluorescence in-situ hybridization; rtPCR, real-time PCR; NGS, Next Generation Sequencing; TKI, Tyrosine Kinase inhibitor.

Alectinib in 2; *METexon14* mutated patients were treated with Crizotinib in 4 cases and Capmatinib in 1. More details are summarized in Table 1.

3.2. cfDNA extraction and sequencing performances

All the 58 patients enrolled were included in the NGS analysis for the determination of the driver mutation detection rate through liquid biopsy. All cfDNA libraries were suitable at qualitative and quantitative controls evaluation.

cfDNA was extracted from an average volume of 4.3 mL (range 2.5–5 mL) of plasma, allowing to obtain on average 27.1 ng per mL of concentration (range 4.3–135 ng per mL). The average total isolated cfDNA mass obtained was 117.2 ng and the average cfDNA input was 43.0 ng (range 9.5–50 ng). We always used the maximum input when available, in 53% of cases input cfDNA was 50 ng (32/58), in 91% of cases input was above 20 ng (53/58). On average, 34.5 million reads were generated from each sample, and the number of reads ranged between 19 and 53 million. The mean sequencing depth was 12,030 (range 6330–17,980). Reads that mapped on target region, defined as target rate, was on average 66.9%. Median unique depth, meaning the depth of unique sequenced DNA fragments, that is, with duplicates removed, was a mean of 5197 unique reads per sample. Theoretical sensitivity or the probability of detecting a variant molecule at the limit of detection (0.5% Allele Frequency) was a mean of 100% across all samples.

3.3. Analysis of positive percent agreement between plasma and tissue specimens

Since all patients in the study population were positive for an oncogenic fusion or *METexon14* mutation tested on tissue specimens, only PPA was evaluated. To perform the PPA analysis between plasma and tissue samples, we sequenced plasma samples obtained from the rearranged or METexone14 mutated patients included in the study. All liquid biopsy specimens were harvested prior to the administration of the first-line therapy with a TKI. Fifty-seven out of 58 (98%) samples were successfully sequenced and analyzed. Only one sample was excluded from the analysis because library sequencing failed. Results are summarized in Table 2.

Considering the overall cohort, we found a PPA of 37% (21 out of 57 samples) between plasma and tissue samples (Fig. 1A). When each gene was considered, the PPA was 36% (13/36) for *ALK*-rearranged, 18% (2/11) for *ROS1*-rearranged, 80% (4/5) for *RET*-rearranged tumors and 40% (2/5) for patients with *METexon14* skipping mutations (Fig. 1B).

In our cohort, 47 out of 57 (82%) samples presented at baseline with at least 1 co-mutation; median number of co-alterations detected was 2 (range 1–9) with a median of 0.27 of allele frequency (AF) percentage. Neither the presence of co-mutations nor the mean AF (mAF) percentage differed between detected and not detected groups ($p = 0.7300$ and $p = 0.4442$, respectively; Fig. 2A and B).

The most prevalent co-mutated gene was Tumor Protein p53 (*TP53*) (12/57; 21%), followed by Adenomatous Polyposis Coli (*APC*) (7/57; 12%) and SMAD family member 4 (*SMAD4*) (6/57; 10%). Samples with *TP53* gene co-mutation belonged mostly to detected group ($p = 0.0154$; Fig. 2C).

3.4. Correlations between driver detection performance and pre-analytical and clinical factors

In order to establish if some of the pre-analytical parameters could influence the performance of the driver detection, we performed a correlation analysis to verify these hypotheses into our cohort. Firstly, we speculated that the driver detection rate could be potentially affected by the total amount of cfDNA used for library preparation, but we did not see any statistically significant difference ($p = 0.056$; Fig. 3A).

Furthermore, we assessed whether the timing between plasma samples storage and NGS analysis had an impact on driver detection performance; to this purpose, we empirically set out a twelve-month cut-off. Also, this pre-analytical parameter did not seem to influence driver detection performance ($p > 0.9999$; Fig. 3B).

Moreover, we also considered some clinical factors such as previous non-TKI therapy, the best tumor response to TKI, type (lung, liver, bone, brain) and number (less than 3 or greater than 3) of metastatic sites, the presence of intra-/extra-thoracic metastasis and evaluated whether they had an impact on driver detection rate. All statistical analyses are summarized in Table 3. Among these, only the presence of extra-thoracic disease seemed to have a positive impact on the driver detection ($p = 0.0049$. Fig. 3C and D).

No statistically significant differences in PFS and OS were found according to driver detection in plasma (Fig. 4A and B).

Among baseline co-alterations, *TP53* mutation was associated with a statistically significant shorter median PFS (*TP53* mutation Yes vs No: 14.0 vs. 23.6 months; $p = 0.047$; Fig. 4C) and a trend in median OS (*TP53* mutation Yes vs. No: 22.7 vs 72.3 months; $p = 0.076$; Fig. 4D). Interestingly, we found that co-mutations in *KRAS* or Neuroblastoma RAS viral oncogene (*NRAS*) genes were associated with a shorter median PFS (median PFS *KRAS/NRAS* mutations Yes vs No: 2.6 vs. 22.3 months; $p = 0.009$; Fig. 4E) and OS (median PFS *KRAS/NRAS* mutations Yes vs No: 5.7 vs. 72.3 months; $p < 0.001$; Fig. 4F).

4. Discussion

Oncogenic fusions of *ALK*, *ROS1* and *RET* genes and mutations of *METexon14* are actionable alterations in advanced NSCLC and specific TKIs for these targets are available in clinical practice [12,13].

Liquid biopsy is a safe, easy-to-collect and fast alternative to tissue sample analysis for both gene mutation as well as gene fusion detection [5]. Several studies supported the use of liquid biopsy in *EGFR* mutated NSCLC, where paired tissue-plasma analysis demonstrated high reliability, expressed in terms of sensitivity and concordance rate [14]. Based on the positive results obtained by liquid biopsy in *EGFR* mutated NSCLC also by our groups [15,16], considering the growing use of NGS in lung cancer liquid biopsy and the limited evidence about the sensitivity of detection of gene fusions and *METexon14* mutations in ctDNA, we conducted three independent studies in Parma and Padova Oncological centers (DYNAMIC, LiMoRe and ARMONY, respectively). These studies aimed to evaluate the PPA between tissue and plasma samples in the determination of these genetic alterations in advanced NSCLC patients.

We collected plasma samples from 58 tissue confirmed *ALK*, *ROS1* or *RET* positive and *METexon14* mutated NSCLC patients before the start of the first TKI treatment. We successfully sequenced 57 out of 58 (98%) ctDNA samples and the driver alteration was detected in 37% of patients, with a different performance according gene fusions/mutations. The worst performance was observed for *ROS1* (18%) and the best one for *RET* (80%). *ROS1*-fusions are considered very difficult to capture through molecular approaches in ctDNA-based liquid biopsy, possibly due to the genomic coordinate features. In fact, *ROS1* fusions involve long intronic regions or repetitive sequences, limiting the detection power; moreover, breakpoints often occur in novel sequences brought in by DNA repair processes. Several strategies were identified in order to enhance the detection of gene fusion such as the increase of the probe coverage of the most common fusion partner genes, the inclusion of extensive tiling of introns and the creation of more optimized bioinformatics pipeline for calling this fusion [17]. Notably, ctDNA-based NGS results from *RET* positive patients revealed a PPA of 80%, which is higher compared to other fusions. At the best of our knowledge, there are no published data that confirm the superiority of *RET* compared to other oncogenic fusions, in terms of driver detection strength. Interestingly, in our cohort *RET* positive patients presented with high disease burden and extra-thoracic metastasis, at the time of study enrollment, probably resulting in an increased ctDNA shedding. Given the low frequency of this driver alteration and the limited number of patients included in our study, no further conclusions are possible. In patients with *ALK* rearrangements

Table 2
Plasma NGS results.

Patients ID	Driver Alteration	Co-mutated genes	Coding Change	Exon Number	Amino Acid Change	% Allele Frequency/CNV score*
ALK-1	–	*SMAD4*	c.380G > T	3	p.C127F	0.22%
		MSH6	c.4054 A > T	10	p.K1352[a]	0.16%
ALK-2	ALK (20):EML4 (13)	-				
ALK-3	–	*TP53*	c.488 A > G	5	p.Y163C	0.15%
		PIK3CA	c.2974C > T	21	p.R992[a]	2.66%
		MTOR	c.7501 A > T	56	p.I2501F	0.15%
		BRAF	c.1003 T > A	8	p.S335T	0.09%
		MAP2K1	c.546G > C	5	p.E182D	0.10%
ALK-4	–	*APC*	c.4901C > G	16	p.P1634R	0.41%
		FGFR2	c.910G > A	7	p.D304 N	0.17%
		RB1	c.2068A > T	20	p.N690Y	0.10%
ALK-5	–	-				
ALK-6	–	*MAP2K2*	c.158G > A	2	p.R53Q	0.27%
		BRCA2	c.6859 A > G	12	p.R2287G	0.29%
ALK-7	ALK (20):EML4 (14)	-				
ALK-8	ALK (20):EML4 (14)	*TP53*	c.659 A > G	6	p.Y220C	0.29%
		GNAS	c.605G > A	8	p.R202H	0.59%
ALK-9	ALK (20):EML4 (13)	*IDH1*	c.401C > A	4	p.A134D	0.05%
		APC	c.1176C > G	10	p.H392Q	51.56%
ALK-10	–	*KRAS*	c.38G > A	2	p.G13D	2.86%
		MTOR	c.5664C > G	40	p.F1888L	0.07%
		STK11	c.977 T > C;	8	p.W308[a]	1.52%
		FLT4	c.923G > A	7	p.I326T	0.07%
ALK-12	–	-				
ALK-13	–	*NRAS*	c.35G > A	2	p.G12D	0.18%
ALK-14	–	*SMAD4*	c.1516G > A	12	p.V506 M	0.11%
ALK-15	–	*PTEN*	c.388C > G	5	p.R130G	0.21%
		BRCA2	c.8351G > A	19	p.R2784Q	42.76%
		CCND1	c.161C > G	1	p.P54R	48.01%
		KDR	c.1052C > A	8	p.P351H	0.08%
		MTOR	c.6790G > A	48	p.E2264K	0.18%
		RET	c.122 A > G	2	p.Y41C	0.07%
ALK-16	ALK (20):EML4 (13)	*TP53*	c.1025G > C	10	p.R342P	0.31%
		PTEN	c.574C > T	6	p.Q192[a]	4.03%
		CDKN2A	c.994-1G > C	1	-p.D24Y	0.23%
		CCND3	c.70G > T	2	p.A128T	6.79%
		BRCA2	c.382G > A	3	p.L152V	46.69%
			c.454C > G	25	p.G3153A	0.13%
			c.9458G > C			55.27%
ALK-17	–	*PTEN*	c.316G > T	5	p.E106[a]	0.17%
ALK-18	–	*CCND2*	c.377 A > G	2	p.Y126C	1.26%
		FGFR2	c.607C > T	5	p.R203C	0.09%
ALK-19	–	-				
ALK-20	–	*FLT3*	c.2505 T > A	20	p.D835E	0.02%
		GNAS	c.605G > A	8	p.R202H	0.11%
		KIT	c.2286G > T	16	p.L762F	0.14%
		MET	c.3730G > T	19	p.A1244S	0.17%
		SMAD4	c.788-2 A > G		–	0.08%
ALK-21	ALK (20):EML4 (13)	*ALK*	c.3172+4 A > T	16	-p.A1571Y	0.09%
		APC	c.4711G > T	7	p.I254F	0.12%
		TP53	c.760 A > T	4	p.E152Q	0.08%
		CD274	c.454G > C	22	p.D1002Y	47.68%
		PDGFRA	c.3004G > T			47.27%
ALK-22	ALK (20):EML4 (13)	*AR*	c.2134C > G	4	p. Q712E	0.1%
		BRCA1	c.2051C > A	10	p. P684Q	0.11%
		ROS1	c.5824C > T	36	p.R1942W	46.40%
ALK-23	–	*SMAD4*	c.842C > A	7	p.P281H	0.09%
ALK-24	–	*TP53*	c.748C > T	7	p.P250S	0.15%
		PDGFRA	c.287G > A	3	p.G96E	0.32%
		AR	c.1174C > T	1	p.P392S	47.49%
ALK-25	–	-				
ALK-26	ALK (20):EML4 (13)	*CDKN2A*	c.238C > T	2	p.R80[a]	0.42%
		PIK3CA	c.3132 T > A	21	p.N1044K	0.05%
		PITCH1	c.3080G > T	18	p.W1027L	0.09%
		TP53	c.536 A > G	5	p.H179R	0.13%
ALK-27	ALK (20):EML4 (6)	*AR*	c.1279C > G	7	p.P427A	0.23%
		ABL1	c.1235 A > T	1	p.T412F	0.05%
ALK-28	–	*KIT*	c.2347C > G	16	p.L783V	0.03%
ALK-29	–	*APC*	c.2701C > T	16	p.Q901[a]	0.3%
		BRAF	c.1906C > T	16	p.Q636[a]	0.36%
		CTNNB1	c.110C > T	3	p.S37F	0.07%
		MAP2K1	c.479G > A	4	p.R160K	0.43%
		MSH2	c.778G > A	4	p.E260K	0.40%
		PIK3CA	c.842C > T	5	p.E281K	0.21%

(*continued on next page*)

Table 2 (*continued*)

Patients ID	Driver Alteration	Co-mutated genes	Coding Change	Exon Number	Amino Acid Change	% Allele Frequency/CNV score*
		SMO	c.859G > T	5	p.G287[a]	0.1%
			c.1093G > A	6	p.E365K	0.05%
			c.920C > T	4	p.T307I	46.34%
ALK-30	ALK (20):EML4 (6)	*KIT*	c.2237C > T	16	p.S746L	0.13%
ALK-31	–	*CFS1R*	c.121C > T	3	p.R41[a]	0.14%
		TSC2	c.217G > T	3	p.G73W	0.17%
		CCND2	c.316 A > G	2	p.M106V	46.90%
		CSF1R	c.2760G > C	21	p.E920D	43.72%
ALK-32	ALK (20):EML4 (6)	*APC*	c.646C > T	7	p.R216[a]	0.36%
ALK-33	ALK (20):EML4 (13)	*APC*	c.6404 T > A	16	p.I2135 N	0.39%
ALK-34	ALK (20):EML4 (13)	*ARAF*	c.949G > A	10	p.G317R	11.33%
		RB1	c.764G > A	8	p.R255Q	25.91%
		ERBB2	c.931 T > C	8	p.C311R	0.03%
		KIT	c.2312G > T	16	p.S771I	0.08%
		SMAD4	c.770C > G	6	p.P257R	0.05%
ALK-35	–	*EGFR*	c.2573 T > G	21	p.L858R	60.87%
		BRCA1	-c.3616G > A	10	amplification	8.39
		CDK6	c.631G > C	5	p.A1206T	0.55%
		JAK3	c.1569G > T	11	p.E211Q	0.13%
		NRAS	c.191 A > G	3	p.W523C	0.06%
		PIK3CA	c.35G > A	2	p.Y64C	0.25%
		VHL	c.1333C > A	8	p.G12D	0.25%
			c.626 A > T	3	p.L445I	0.05%
					p.Q209L	0.26%
ALK-36	–	*KRAS*	c.34G > T	2	p.G12C	0.31%
ALK-37	–	*NFE2L2*	c.85G > A	2	p.D29 N	0.33%
		BRCA1	c.2578 A > G	10	p.T860A	0.07%
		EGFR	c.2996G > A	25	p.R999H	0.08%
		APC	c.1220 T > G	10	p.L407R	0.08%
ROS-1	–	*JAK2*	c.1849G > T	14	p.V617F	0.34%
		CSF1R	c.1237G > A	9	p.G413S	47.20%
ROS-2	–	*PIK3CA*	c.1088G > C	6	p.G363A	0.16%
ROS-3	ROS1(34):CD74 (6)	*TP53*	c.833C > T	8	p.P278L	3.17%
		SMAD4	c.988G > A	9	p.E330K	3.11%
		FBXW7	c.529G > A	3	p.E177K	1.86%
		CCND2	c.275C > T	2	p.P92L	2.72%
		AR	c.1904T > C	4	p.L635P	0.60%
ROS-4	–	*SMO*	c.2314C > T	12	p.R772C	46.04%
ROS-5	–	*FLT1*	c.3104 T > C	23	p.V1035A	0.07%
		BRCA2	c.9976 A > T	27	p.K3326[a]	47.25%
ROS-6	ROS1(34):CD74 (6)	*MET*	c.3082+2 T > A	14	-p.A344V	0.04%
		FGFR2	c.1031C > T	8		0.39%
ROS-7	–	*BRCA1*	c.1718C > T	10	p.S573L	48.54%
ROS-8	–	*ALK*	c.3271G > A	20	p.D1091 N	0.06%
		FLT1	c.3271G > A	19	p.E865G	0.12%
ROS-9	–	-				
ROS-10	–	*MSH2*	c.2635-3C > T	8	-p.R280T	1.03%
		TP53	c.839G > C	6	p.R213[a]	0.62%
		STK11	c.637C > T	9	p.K319 N	0.94%
		ALK	c.957G > C	5	p.D207H	0.43%
		PTEN	c.619G > C	6	-p.H196 N	0.99%
			c.1414+1G > A			0.21%
			c.586C > A			0.33%
ROS-11	–	*CDKN2A*	c.358G > T	2	p.E120[a]	0.28%
		FGFR1	c.802G > A	7	p.G268S	0.29%
		PTEN	c.968dupA	8	p.N323fs	0.12%
RET-1	KIF5B(15):RET (12)	*FBXW7*	c.671G > A	4	p.R224Q	0.08%
RET-2	RET (12):ERC1 (8)	*TP53*	c.469G > T	5	p.V157F	16.33%
		CDK4	c.71G > T	2	p.R24L	16.24%
RET-3	–	-				
RET-4	KIF5B(23):RET (12)	-				
RET-5	KIF5B(15):RET (12)	*ESR1*	c.1712C > T	10	p.A571V	1.01%
		FGFR1	c.1397C > T	11	p.A466V	0.70%
		TP53	c.524G > A	5	p.R175H	23.24%
		RET	c.991C > T	9	p.Q331[a]	23.55%
		MSH2	c.2533G > T	14	p.A845S	21.32%
		FLT1	c.46G > T	1	p.E16[a]	24.20%
		KEAP1	c.2749C > G	20	p.L917V	19.29%
		KIT	c.482 T > G	2	p.M161R	33.25%
			c.2614G > C	19	p.G872R	31.82%
METex14-1	MET exon 14 p.D1028H	*MET*	c.3082G > C	14	p.D1028H	0.06%
		PMS2	c.2324 A > G	14	p.N775S	5.43%
METex14-2	–	*TP53*	c.578 A > G	6	p.H193R	0.08%
		RB1	c.1597G > T	17	p.E533[a]	0.17%
		CSFR1	c.2320-3C > A		–	0.13%
METex14-3	MET exon 14 c.3082+3 A > G	*MET*	c.3082+3 A > G	14	-p.Y236C	0.35%

(*continued on next page*)

Table 2 (*continued*)

Patients ID	Driver Alteration	Co-mutated genes	Coding Change	Exon Number	Amino Acid Change	% Allele Frequency/CNV score*
		TP53	c.707 A > G	7	p.R552[a]	0.52%
		RB1	c.1654C > T	17	p.K447I	0.91%
		ESR1	c.1340 A > T	1	-p.E341[a]	0.13%
		PIK3R1	c.*109 T > A	9	–	0.09%
		ROS1	c.1021G > T	1		0.56%
			c.124-2 A > G			0.07%
METex14-4	–	-				
METex14-5	–	*PMS2*	c.2324 A > G	14	p.N775S	8.39%

SRV, splice region variant; CNV, copy number variation.

[a] The CNV score is a statistical summary of a called amplification that takes into account the log2 ratio to normal copy number and the standard error of that estimate.

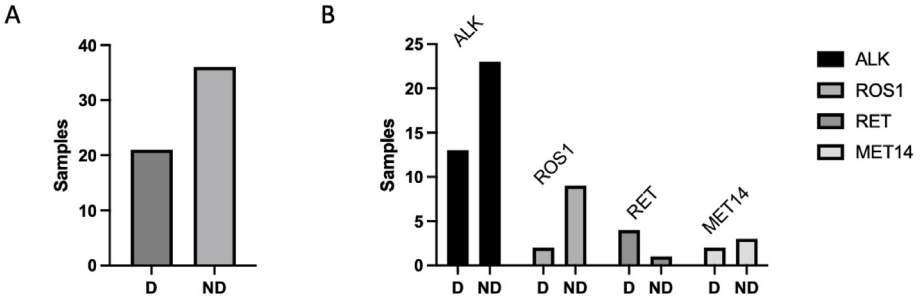

Fig. 1. PPA between tissue and plasma samples. A) Concordance analysis in the overall cohort. B) Concordance analysis grouped by specific gene. D, driver alteration detected; ND, driver alteration not detected.

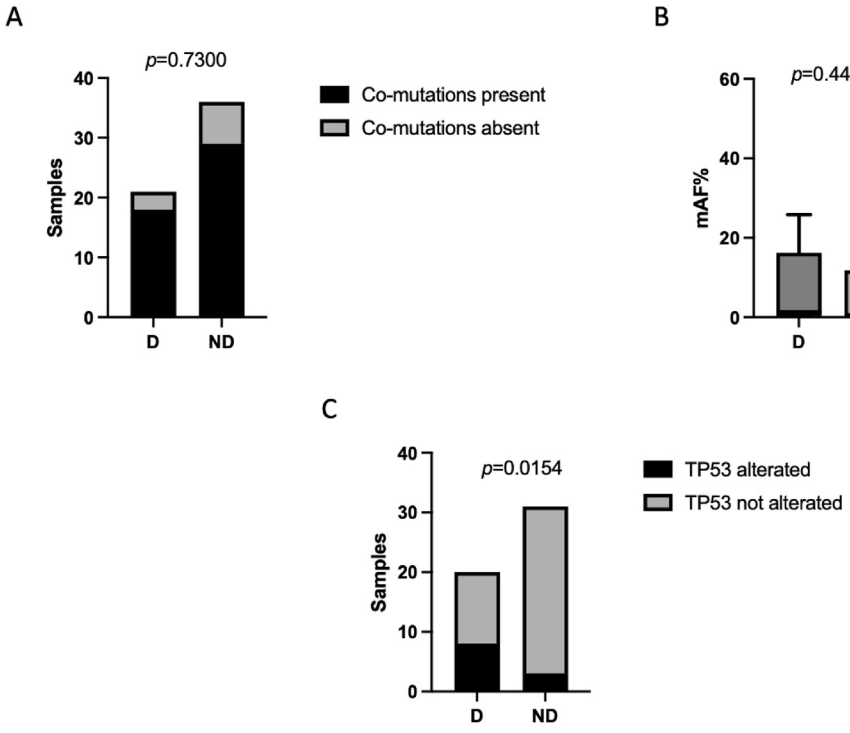

Fig. 2. Impact of co-alterations and allele frequency on driver detection performance. A) Mann-Whitney test between co-alterations status at baseline and driver detection performance. B) Mann-Whitney test between mAF% per sample and driver detection performance. C) Fisher's exact test considering the effect of TP53 co-altered gene on driver detection performance. Significant values are reported when $p < 0.05$. D, driver alteration detected; ND, driver alteration not detected; mAF, mean allele frequency.

detected through blood-based NGS, encouraging results from the BFAST study paved the way for the clinical utility of ctDNA-based NGS in *ALK*-positive NSCLC patients [18].

Overall, our results are consistent with already published data, in which detection rate of gene rearrangements is lower (range 0–70.5%) in ctDNA samples, compared to other DNA-based alterations [17,19–25]. In order to explain this difference in sensitivity we should look beyond the shedding status. Indeed, several plasma samples of our cohort displayed somatic single nucleotide variants (SNVs) in the absence of the oncogenic fusion, suggesting impaired sensitivity, specifically for the oncogenic fusion and *METexon14* mutations and not for DNA point mutations. Our results are in line with the study of McCoach et al., which identified *ALK* resistance mutations without *ALK* fusion detection, using Guardant 360 NGS panel [26]. As mentioned before, in the context of genetic fusions hybrid-capture probe design and accurate analytical pipelines are essential, due to the great variability existing among breakpoint positions and the fragmented nature of cfDNA.

Furthermore, another aspect to consider explaining the low efficiency

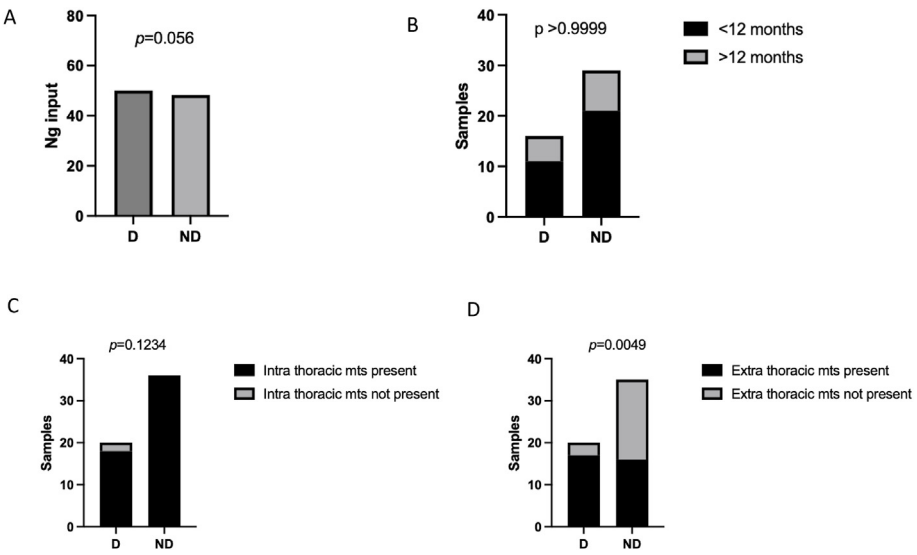

Fig. 3. Impact of pre-analytical and clinical factors on driver detection performance. A) Mann-Whitney test between input cfDNA and driver detection performance. B) Fisher's exact test between NGS analysis timing and driver detection performance. C) Fisher's exact test between the presence of intra-thoracic disease and driver detection performance. D) Fisher's exact test between the presence of extra-thoracic disease and driver detection performance. Significant values are reported when $p < 0.05$. D, driver alteration detected; ND, driver alteration not detected; mts, metastasis.

Table 3
Statistical analysis performed among clinical parameters and driver detection performance.

Type of Correlation	p value
Previous non-TKI therapy *vs.* driver detection efficiency	>0.9999
Best tumor response to TKI *vs.* driver detection performance	0.4880
Number of mts sites *vs.* driver detection performance	0.2738
Lung mts *vs.* driver detection performance	0.4173
Liver mts *vs.* driver detection performance	0.3267
Bone mts *vs.* driver detection performance	0.1082
Brain mts *vs.* driver detection performance	0.4729
Intra-thoracic disease *vs.* driver detection performance	0.1234
Extra-thoracic disease *vs.* driver detection performance	0.0049

Mts, metastasis; ns, not statistically significant correlation.

in fusion detection is the tumor fraction (TF). In the presence of a high TF (≥10%), the probability to have a concordant result between blood and tissue is very high [27]. In this study, we performed NGS analysis with the commercially available AVENIO ctDNA Expanded kit, which does not estimate the TF in extracted cfDNA, unlike the NGS panels Guardant360® CDx and FoundationOne® Liquid CDx. We hypothesize that some of our plasma samples may lack adequate ctDNA content. Consistent with our hypothesis, recent research dedicated to detection of gene fusions in liquid biopsy found a more compatible prevalence of gene fusions in samples with TF ≥ 1% compared to samples with inferior TF [10]. Indeed, the Avenio panel sensitivity for fusions is certified down to 1%, while, in our experience it has proven to be much more sensitive for SNV, far below the 0.5% detection limit stated by the manufacturer. We hypothesize that the relatively low concordance rate in our study is due to concomitant technical and biological reasons including low level of ctDNA shedding and limited sensitivity of current DNA-based NGS technology for fusion detection.

Cell-free RNA (cfRNA) is being investigated as a biomarker in the detection of gene fusions and rearrangements, as a replacement or as a complementary tool to cfDNA. RNA-based approaches allow to avoid the sequencing of intronic regions and led to profile highly expressed transcripts, thus achieving greater sensitivity compared to cfDNA. Data have already been published in literature and confirm this assumption [24,28,29]. Despite these encouraging results, cfRNA remains a more difficult analyte to handle and none of the globally available cfRNA-based approaches have yet gained FDA-approval for use in clinical molecular diagnosis. Therefore, where possible it could be desirable to combine the profiling results of both cfDNA and cfRNA analytes for a more complete and confident molecular diagnosis.

In our study cohort, the genetic co-mutation most frequently detected involved *TP53* gene (21% of patients) followed by *APC* and *SMAD4* (12% and 10%, respectively). The clinical significance of co-alterations in this setting is less characterized than DNA SNVs [30,31]. However, it is known that rearranged NSCLC patients harbor *TP53* aberrations less frequently than NSCLC with point mutations [32,33]. Similarly to *EGFR* mutated NSCLC [34], also in our cohort we observed shorter PFS in *TP53* blood positive vs. negative patients; moreover, *TP53* co-mutations were predominantly present in the detected samples suggesting a more aggressive phenotype with a greater probability of releasing ctDNA. Furthermore, a significantly worst outcome was observed in patients harboring co-occurring plasmatic *KRAS* or *NRAS* point mutations, as previously reported [35,36].

If main pre-analytical variables did not influence the driver detection rate, among clinical factors, a significant difference between patients with intra- or extra-thoracic disease was found, with a higher driver detection rate in patients with metastasis outside the thorax. This data is consistent with several studies reporting that different sites of disease, such as intra-thoracic or central nervous system metastases, could impair sensitivity of plasma genotyping [17,37–39].

Our study presents some limitations that should be considered. Firstly, the cohort size was relatively small due to the low frequency of oncogenic fusion among NSCLC patients. Second, we could not perform positive and negative predictive value since our cohort included only patients known to have an oncogenic fusion, hence only PPA could be assessed. Finally, with regard to *TP53* co-mutations, since we did not analyze matched leucocyte DNA, we cannot rule out that some of them may derive from clonal hematopoiesis [40]. Larger studies, involving either RNA or DNA based approaches, are needed to comprehensively assess the role of liquid biopsy in the molecular diagnosis of NSCLC patients.

5. Conclusions

In conclusion, our study confirms that ctDNA testing to detect oncogenic fusions or *METexon14* mutations in advanced NSCLC patients is useful, even if type of gene alterations and clinical characteristics could influence the driver detection rate. If liquid biopsy represents a complementary tool to tissue genotyping, however, as demonstrated by our results, more sensitive approaches for gene fusions and *METexon14* detection are needed to implement its strength and reliability.

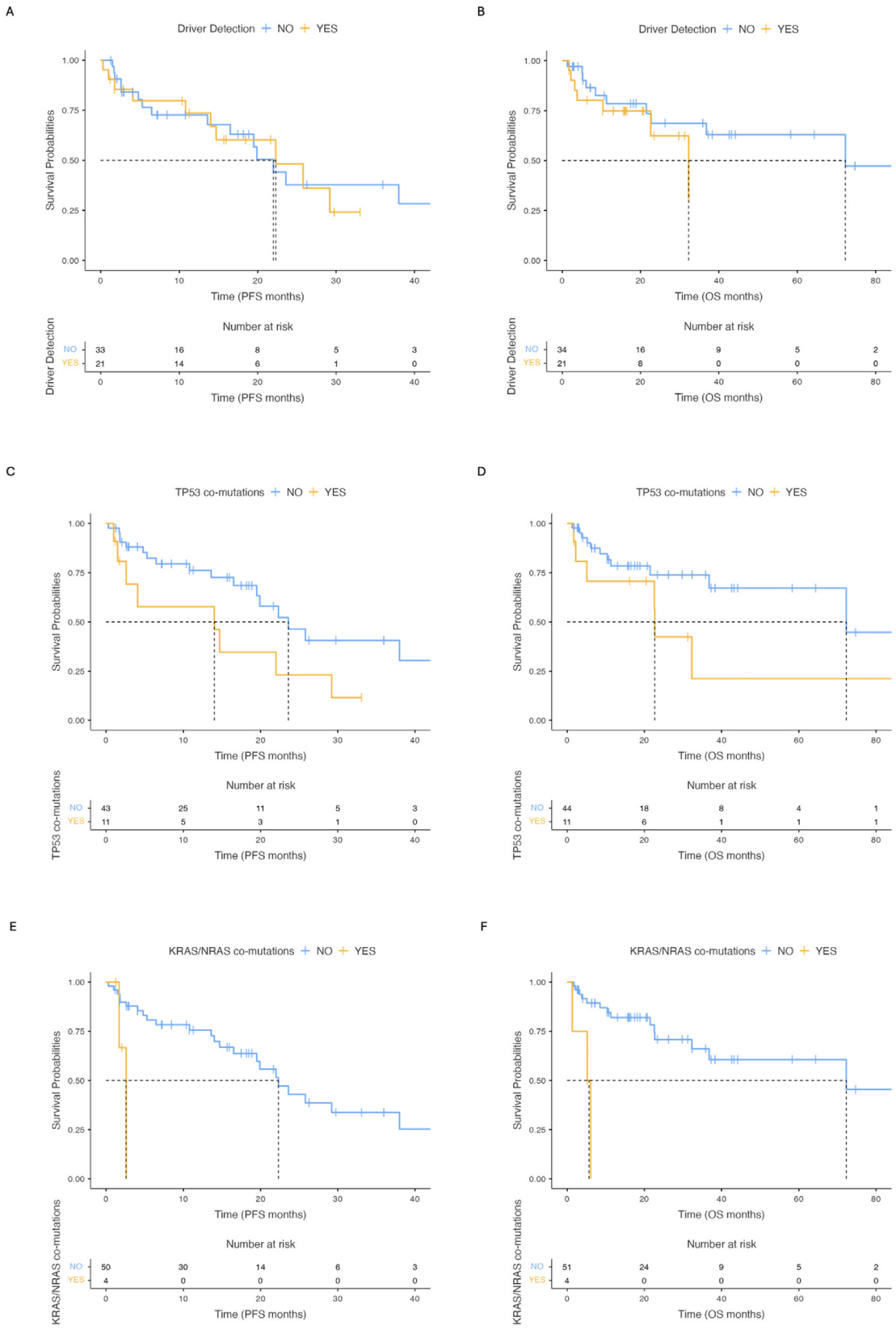

Fig. 4. Kaplan-Meier curves for A) Progression-free survival (PFS) and B) Overall survival (OS) according to driver detection, for C) PFS and D) OS according to *TP53* co-mutation at baseline and for E) PFS and F) OS according to *KRAS/NRAS* co-mutation at baseline.

Funding

In Parma Center (LiMoRe project) this work was supported by Roche Foundation "Roche per la Ricerca 2020". Institutional Grant by Istituto Oncologico Veneto IRCCS (5x1000 Cancerplat2 and Ricerca Corrente 2021).

Authors' contribution

Conceptualization and design: Marcello Tiseo, Stefano Indraccolo, Giulia Pasello, Paola Bordi, Roberta Minari. Literature research, data accumulation and interpretation: Michela Verzè;, Andrea Boscolo Bragadin, Fabiana Perrone, Daniela Scattolin, Paola Bordi, Monica Pluchino, Alessandro Leonetti, Giulia Mazzaschi, Francesco Bonatti, Laura Bonanno. Investigation and laboratory analysis: Andrea Boscolo Bragadin, Elisabetta Zulato, Giorgia Nardo, Chiara Dalle Fratte, Alessia Padovan, Monica Pluchino, Francesco Bonatti. Manuscript writing and original draft preparation: Michela Verzè;, Andrea Boscolo Bragadin, Fabiana Perrone, Daniela Scattolin. Manuscript Supervision: Marcello Tiseo, Stefano Indraccolo, Giulia Pasello, Roberta Minari. Formal Analysis: Michela Verzè;, Andrea Boscolo Bragadin. Figure and Tables preparation: Michela Verzè;, Andrea Boscolo Bragadin. Critical Review and Editing: All the authors. All authors have read and approved to the submitted version of the manuscript.

Declaration of competing interest

The authors declare the following financial interests/personal relationships which may be considered as potential competing interests:

Giulia Pasello reports financial support and article publishing charges were provided by Veneto Oncology Institute. Marcello Tiseo reports financial support was provided by University Hospital of Parma. Marcello Tiseo reports a relationship with Astra-Zeneca, Pfizer, Eli-Lilly, BMS, Novartis, Roche, MSD, Boehringer Ingelheim, Otsuka, Takeda, Pierre Fabre, Amgen, Merck, Sanofi, Janssen, Daiichi Sankyo that includes: consulting or advisory and speaking and lecture fees. Marcello Tiseo reports a relationship with Astra-Zeneca, Boehringer Ingelheim. That includes: funding grants. Giulia Pasello reports a relationship with Astra-Zeneca, Amgen, BMS, Eli Lilly, Janssen, MSD, Novartis, Roche that includes: consulting or advisory and speaking and lecture fees. Giulia Pasello reports a relationship with Astra-Zeneca, Roche, MSD that includes: funding grants. Laura Bonanno reports a relationship with Astra-Zeneca, MSD, BMS, Roche, Novartis, Eli-Lilly that includes: consulting or advisory and speaking and lecture fees. Laura Bonanno reports a relationship with Astra-Zeneca. That includes: funding grants. If there are other authors, they declare that they have no known competing financial interests or personal relationships that could have appeared to influence the work reported in this paper.

References

[1] Barta JA, Powell CA, Wisnivesky JP. Global epidemiology of lung cancer. Ann Glob Health 2019. https://doi.org/10.5334/aogh.2419.
[2] Hendriks LE, et al. Oncogene-addicted metastatic non-small-cell lung cancer: ESMO Clinical Practice Guideline for diagnosis, treatment and follow-up. Ann Oncol Apr. 2023;34(4):339–57. https://doi.org/10.1016/j.annonc.2022.12.009.
[3] Siravegna G, Marsoni S, Siena S, Bardelli A. Integrating liquid biopsies into the management of cancer. Nat Rev Clin Oncol 2017;14(9):531–48. https://doi.org/10.1038/nrclinonc.2017.14.
[4] Bonanno L, et al. Liquid biopsy and non-small cell lung cancer: are we looking at the tip of the iceberg? Br J Cancer 2022;127(3):383–93. https://doi.org/10.1038/s41416-022-01777-8.
[5] Rolfo C, et al. Liquid biopsy for advanced non-small cell lung cancer (NSCLC): a statement paper from the IASLC. J Thorac Oncol Sep. 2018;13(9):1248–68. https://doi.org/10.1016/j.jtho.2018.05.030.
[6] Schrock AB, et al. Hybrid capture–based genomic profiling of circulating tumor DNA from patients with advanced non–small cell lung cancer. J Thorac Oncol 2019; 14(2):255–64. https://doi.org/10.1016/j.jtho.2018.10.008.
[7] Papadopoulou E, et al. "Clinical feasibility of NGS liquid biopsy analysis in NSCLC patients,". PLoS One Dec. 2019;14(12):e0226853. https://doi.org/10.1371/journal.pone.0226853 [Online]. Available.
[8] U.S. Food and Drug Administration. Guardant360 CDx. https://www.fda.gov/medical-devices/recently-approved-devices/guardant360-cdx-p200010s008.".
[9] U.S. Food and Drug Administration. FoundationOne Liquid CDx. https://www.fda.gov/medical-devices/recently-approved-devices/foundationone-liquid-cdx-f1-liquid-cdx-p190032s010.".
[10] Kasi PM, et al. "Circulating tumor DNA enables sensitive detection of actionable gene fusions and rearrangements across cancer types,". Clin Cancer Res Dec. 2023. https://doi.org/10.1158/1078-0432.CCR-23-2693.
[11] V Tavtigian S, Harrison SM, Boucher KM, Biesecker LG. Fitting a naturally scaled point system to the ACMG/AMP variant classification guidelines. Hum Mutat Oct. 2020;41(10):1734–7. https://doi.org/10.1002/humu.24088.
[12] Harada G, Yang S-R, Cocco E, Drilon A. Rare molecular subtypes of lung cancer. Nat Rev Clin Oncol 2023;20(4):229–49. https://doi.org/10.1038/s41571-023-00733-6.
[13] Remon J, et al. MET alterations in NSCLC-current perspectives and future challenges. J Thorac Oncol Apr. 2023;18(4):419–35. https://doi.org/10.1016/j.jtho.2022.10.015.
[14] Wang Naiqun, Zhang Xialolian, Wang Feilong, Zhang Min, Sun Bo, Lu Wei. The diagnostic accuracy of liquid biopsy in EGFR-mutated NSCLC: a systematic review and meta-analysis of 40 studies. SLAS Technol Feb. 2021;1:42–54. https://doi.org/10.1177/2472630320939565.
[15] Dal Maso A, et al. "Clinical features and progression pattern of acquired t790m-positive compared with t790m-negative EGFR mutant non-small-cell lung cancer: catching tumor and clinical heterogeneity over time through liquid biopsy,". Clin Lung Cancer Jan. 2020;21(1):1–14. https://doi.org/10.1016/j.cllc.2019.07.009. e3.
[16] Minari R, et al. Detection of EGFR-activating and T790M mutations using liquid biopsy in patients with EGFR-mutated non-small-cell lung cancer whose disease has progressed during treatment with first- and second-generation tyrosine kinase inhibitors: a multicenter real-life retrospective study. Clin Lung Cancer Sep. 2020; 21(5):e464–73. https://doi.org/10.1016/j.cllc.2020.02.021.
[17] Dagogo-Jack I, et al. Molecular analysis of plasma from patients with ROS1-positive NSCLC. J Thorac Oncol May 2019;14(5):816–24. https://doi.org/10.1016/j.jtho.2019.01.009.
[18] Dziadziuszko R, et al. Blood first assay screening trial (BFAST) in treatment-naive advanced or metastatic NSCLC: initial results of the phase 2 ALK-positive cohort. J Thorac Oncol 2021;16(12):2040–50. https://doi.org/10.1016/j.jtho.2021.07.008.
[19] Paturu R, et al. Non-small cell lung cancer: targetable variants in concurrent tissue and liquid biopsy testing in a north Indian cohort. Asian Pac J Cancer Prev APJCP 2023;24(10):3467–75. https://doi.org/10.31557/APJCP.2023.24.10.3467.
[20] Noé J, et al. Concordance between tissue ALK detection by immunohistochemistry and plasma ALK detection by next-generation sequencing in the randomized phase 3 ALEX study in patients with treatment-naive advanced ALK-positive NSCLC. JTO Clin Res Rep Jul. 2022;3(7). https://doi.org/10.1016/j.jtocrr.2022.100341.
[21] Raez LE, et al. Liquid biopsy versus tissue biopsy to determine front line therapy in metastatic non-small cell lung cancer (NSCLC). Clin Lung Cancer Mar. 2023;24(2): 120–9. https://doi.org/10.1016/j.cllc.2022.11.007.
[22] Supplee JG, et al. Sensitivity of next-generation sequencing assays detecting oncogenic fusions in plasma cell-free DNA. Lung Cancer Aug. 2019;134:96–9. https://doi.org/10.1016/j.lungcan.2019.06.004.
[23] Kwon M, et al. Longitudinal monitoring by next-generation sequencing of plasma cell-free DNA in ALK rearranged NSCLC patients treated with ALK tyrosine kinase inhibitors. Cancer Med Aug. 2022;11(15):2944–56. https://doi.org/10.1002/cam4.4663.
[24] Hasegawa N, et al. Highly sensitive fusion detection using plasma cell-free RNA in non-small-cell lung cancers. Cancer Sci Oct. 2021;112(10):4393–403. https://doi.org/10.1111/cas.15084.
[25] Sugimoto A, et al. A large-scale prospective concordance study of plasma- and tissue-based next-generation targeted sequencing for advanced non–small cell lung cancer (LC-SCRUM-Liquid). Clin Cancer Res Apr. 2023;29(8):1506–14. https://doi.org/10.1158/1078-0432.CCR-22-1749.
[26] McCoach CE, et al. Clinical utility of cell-free DNA for the detection of ALK fusions and genomic mechanisms of ALK inhibitor resistance in non–small cell lung cancer. Clin Cancer Res Jun. 2018;24(12):2758–70. https://doi.org/10.1158/1078-0432.CCR-17-2588.
[27] Husain H, et al. "Tumor fraction correlates with detection of actionable variants across > 23,000 circulating tumor DNA samples,". JCO Precis Oncol Oct. 2022;6: e2200261. https://doi.org/10.1200/PO.22.00261.
[28] Choudhury Y, et al. A cell-free RNA-based next-generation sequencing (NGS) assay for the detection of actionable gene fusions in patients with non–small cell lung cancer (NSCLC). J Clin Oncol Jun. 2022;40(16_suppl):3040. https://doi.org/10.1200/JCO.2022.40.16_suppl.3040.
[29] Giménez-Capitán A, et al. Detecting ALK, ROS1, and RET fusions and the METΔex14 splicing variant in liquid biopsies of non-small-cell lung cancer patients using RNA-based techniques. Mol Oncol Sep. 2023;17(9):1884–97. https://doi.org/10.1002/1878-0261.13468.
[30] Nardo G, et al. Detection of low-frequency KRAS mutations in cfDNA from EGFR-mutated NSCLC patients after first-line EGFR tyrosine kinase inhibitors. Front Oncol 2021;10 [Online]. Available, https://www.frontiersin.org/articles/10.3389/fonc.2020.607840.
[31] Alberto Pavan, Bragadin Andrea Boscolo, Lorenzo Calvetti, Bonanno Laura. Role of next generation sequencing-based liquid biopsy in advanced non-small cell lung cancer patients treated with immune checkpoint inhibitors: impact of STK11, KRAS

and TP53 mutations and co-mutations on outcome. Transl Lung Cancer Res 2021 Jan;10(1):202–20. https://doi.org/10.21037/tlcr-20-674.
[32] Michels S, et al. Clinicopathological characteristics of RET rearranged lung cancer in European patients. J Thorac Oncol Jan. 2016;11(1):122–7. https://doi.org/10.1016/j.jtho.2015.09.016.
[33] Kron A, et al. Impact of TP53 mutation status on systemic treatment outcome in ALK-rearranged non-small-cell lung cancer. Ann Oncol Oct. 2018;29(10):2068–75. https://doi.org/10.1093/annonc/mdy333.
[34] Vokes NI, et al. Concurrent TP53 mutations facilitate resistance evolution in EGFR-mutant lung adenocarcinoma. J Thorac Oncol Jun. 2022;17(6):779–92. https://doi.org/10.1016/j.jtho.2022.02.011.
[35] Mengoli MC, Barbieri F, Bertolini F, Tiseo M, Rossi G. K-RAS mutations indicating primary resistance to crizotinib in ALK-rearranged adenocarcinomas of the lung: report of two cases and review of the literature. Lung Cancer Mar. 2016;93:55–8. https://doi.org/10.1016/j.lungcan.2016.01.002.
[36] Bordi P, et al. Detection of ALK and KRAS mutations in circulating tumor DNA of patients with advanced ALK-positive NSCLC with disease progression during crizotinib treatment. Clin Lung Cancer Nov. 2017;18(6):692–7. https://doi.org/10.1016/j.cllc.2017.04.013.
[37] Oxnard GR, et al. Association between plasma genotyping and outcomes of treatment with osimertinib (AZD9291) in advanced non–small-cell lung cancer. J Clin Oncol Jun. 2016;34(28):3375–82. https://doi.org/10.1200/JCO.2016.66.7162.
[38] Krug AK, et al. Improved EGFR mutation detection using combined exosomal RNA and circulating tumor DNA in NSCLC patient plasma. Ann Oncol Mar. 2018;29(3):700–6. https://doi.org/10.1093/annonc/mdx765.
[39] Zulato E, et al. Longitudinal liquid biopsy anticipates hyperprogression and early death in advanced non-small cell lung cancer patients treated with immune checkpoint inhibitors. Br J Cancer 2022;127(11):2034–42. https://doi.org/10.1038/s41416-022-01978-1.
[40] Ting Chan Hiu, Ming Chin Yoon, Nakamura Yusuke, Siew-Kee Low. “Clonal hematopoiesis in liquid biopsy: from biological noise to valuable clinical implications,”. Cancers 2020.